A Highly Ca^{2+}-sensitive Pool of Granules Is Regulated by Glucose and Protein Kinases in Insulin-secreting INS-1 Cells

Yan Yang[3] and Kevin D. Gillis[1,2,3]

[1]Department of Biological Engineering, [2]Department of Medical Pharmacology and Physiology, and [3]Dalton Cardiovascular Research Center, University of Missouri-Columbia, Columbia, MO 65211

ABSTRACT We have used membrane capacitance measurements and carbon-fiber amperometry to assay exocytosis triggered by photorelease of caged Ca^{2+} to directly measure the Ca^{2+} sensitivity of exocytosis from the INS-1 insulin-secreting cell line. We find heterogeneity of the Ca^{2+} sensitivity of release in that a small proportion of granules makes up a highly Ca^{2+}-sensitive pool (HCSP), whereas the bulk of granules have a lower sensitivity to Ca^{2+}. A substantial HCSP remains after brief membrane depolarization, suggesting that the majority of granules with high sensitivity to Ca^{2+} are not located close to Ca^{2+} channels. The HCSP is enhanced in size by glucose, cAMP, and a phorbol ester, whereas the Ca^{2+}-sensitive rate constant of exocytosis from the HCSP is unaffected by cAMP and phorbol ester. The effects of cAMP and phorbol ester on the HCSP are mediated by PKA and PKC, respectively, because they can be blocked with specific protein kinase inhibitors. The size of the HCSP can be enhanced by glucose even in the presence of high concentrations of phorbol ester or cAMP, suggesting that glucose can increase granule pool sizes independently of activation of PKA or PKC. The effects of PKA and PKC on the size of the HCSP are not additive, suggesting they converge on a common mechanism. Carbon-fiber amperometry was used to assay quantal exocytosis of serotonin (5-HT) from insulin-containing granules following preincubation of INS-1 cells with 5-HT and a precursor. The amount or kinetics of release of 5-HT from each granule is not significantly different between granules with higher or lower sensitivity to Ca^{2+}, suggesting that granules in these two pools do not differ in morphology or fusion kinetics. We conclude that glucose and second messengers can modulate insulin release triggered by a high-affinity Ca^{2+} sensor that is poised to respond to modest, global elevations of $[Ca^{2+}]_i$.

KEY WORDS: exocytosis • membrane capacitance • amperometry • caged calcium • PKC

INTRODUCTION

Glucose triggers insulin release from pancreatic β cells by closing ATP/ADP-gated K^+ channels, which leads to membrane depolarization, Ca^{2+} influx through voltage-gated Ca^{2+} channels, and $[Ca^{2+}]_i$-triggered exocytosis of insulin-containing granules. Glucose also promotes exocytosis from β cells independently from effects on K^+(ATP) channels (Eliasson et al., 1997; Takahashi et al., 1999; Rosengren et al., 2002). For example, elevated ATP levels may increase the number of vesicles in a readily releasable state. Activation of protein kinases such as cAMP-dependent protein kinase (PKA; Jones et al., 1986; Ammala et al., 1993a; Gillis and Misler, 1993; Rosengren et al., 2002) and PKC (Jones et al., 1985; Ammala et al., 1994) modulate Ca^{2+}-triggered exocytosis from β cells and thus provides a mechanism for hormonal modulation of insulin secretion through second messengers (for review see Jones and Persaud, 1998).

A combination of patch-clamp techniques with photorelease of caged Ca^{2+} allows the Ca^{2+} sensitivity of exocytosis to be directly measured. With these techniques, individual steps in the stimulus–secretion cascade can be isolated so that the detailed mechanisms whereby second messengers modulate exocytosis can be determined. Previous studies using caged Ca^{2+} in β cells show that the Ca^{2+} sensitivity of exocytosis is relatively low such that $[Ca^{2+}]_i > 25$ μM is necessary to elicit rates of exocytosis similar to those measured during voltage-clamp depolarization (Barg et al., 2001). Thus, insulin granules are postulated to be located very close to Ca^{2+} channels in order to sense high $[Ca^{2+}]_i$ levels during Ca^{2+} influx (also see Wiser et al., 1999).

We have recently reported heterogeneity in the Ca^{2+} sensitivity of exocytosis in adrenal chromaffin cells. In particular, we found a highly Ca^{2+}-sensitive pool (HCSP) of granules that can be released at $[Ca^{2+}]_i$ levels in the low μM range (Yang et al., 2002). Here we investigate the Ca^{2+} sensitivity of exocytosis in the INS-1 insulin-secreting cell line. INS-1 cells, like primary β cells, undergo Ca^{2+}-triggered exocytosis of insulin that is modulated by hormones, glucose, and protein kinases (Asfari et al., 1992; Rosengren et al., 2002). We find

Address correspondence to Kevin Gillis, Dalton Cardiovascular Research Center, University of Missouri-Columbia, Research Park Dr., Columbia, MO 65211. Fax: (573) 884-4232; email: gillisk@missouri.edu

Abbreviations used in this paper: HCSP, highly Ca^{2+}-sensitive pool; IRP, immediately releasable pool; PKI, PKA inhibitory peptide; RRP, readily releasable pool.

J. Gen. Physiol. © The Rockefeller University Press • 0022-1295/2004/12/641/11 $8.00
Volume 124 December 2004 641–651
http://www.jgp.org/cgi/doi/10.1085/jgp.200409081

that INS-1 cells have an HCSP in addition to the less Ca^{2+}-sensitive readily releasable pool (RRP) that has previously been characterized. We find that the size of the HCSP in INS-1 cells, but not the Ca^{2+}-sensitive rate constant of release, is increased by glucose and agents that activate PKA and PKC. The HCSP may be responsible for release of insulin that is not tightly coupled to Ca^{2+} influx through Ca^{2+} channels.

MATERIALS AND METHODS

Cell Preparation and Solutions

Rat insulinoma INS-1 cells (provided by C. Wollheim, University of Geneva, Geneva, Switzerland) were maintained in culture media consisting of RPMI 1640 medium supplemented with 50 μM 2-mercaptoethanol, 2 mM L-glutamine, 10 mM HEPES, 100 U/ml penicillin, 100 μg/ml streptomycin, 1 mM pyruvate, and 10% FBS. Cells were kept in a humidified 37°C incubator with 5% CO_2 and were passaged by trypsinization and subcultured once a week. Cell suspensions were plated onto glass coverslips (25 mm OD) coated with 0.3 mg/ml poly D-lysine. Experiments were performed 1 or 2 d after cells were plated out.

The standard bath solution consisted of (in mM) 140 NaCl, 5.5 KCl, 1 $MgCl_2$, 5 $CaCl_2$, 10 HEPES titrated to pH 7.2 with NaOH. The bath solution contained 2.6 mM glucose, whereas higher glucose concentrations were achieved by adding an appropriate volume of a 1 M glucose stock solution. Standard pipette solution consisted of (in mM) 110 L-glutamic acid, 110 *N*-methylglucamine, 8 NaCl, 1 $MgCl_2$, 2 Na_2-ATP, and 40 HEPES titrated to pH 7.2 with CsOH. The Ca^{2+} indicator dyes fura-2FF (K^+ salt; Teflabs) and bisfura-2 (K^+ salt; Molecular Probes) were included in the pipette solution at an equimolar ratio (0.1 mM) to allow measurement of $[Ca^{2+}]_i$ over a wide dynamic range (Voets, 2000). The Ca^{2+} cage Nitrophenyl-EGTA (0.5–1 mM; Ellis-Davies and Kaplan, 1994), 80% loaded with $CaCl_2$, was added to the pipette solution. We adjusted the amount of added $CaCl_2$ and Nitrophenyl-EGTA to achieve baseline $[Ca^{2+}]_i$ values typically in the range of 0.5–0.7 μM. Elevated basal $[Ca^{2+}]_i$ is commonly used in caged Ca^{2+} experiments in order to increase the size of the RRP (e.g., Voets, 2000) and we observed that the HCSP was often quite small or absent when basal $[Ca^{2+}]_i$ was $<\sim$200 nM (not depicted). The rate of C_m increase after achieving the whole-cell configuration was typically 1 fF/s or less and amperometric events were rarely observed (not depicted), thus the "basal" rate of exocytosis appeared to be low before stimulation.

All chemicals were from Sigma-Aldrich except otherwise indicated. PKA inhibitory peptide (PKI) was from Alexis. Bisindoylymaleimide I was from Calbiochem.

$[Ca^{2+}]_i$ Calibration

The Ca^{2+} indicator combination was calibrated in cells using whole-cell recording in a manner similar to that used by Voets (2000). Eight solutions with free $[Ca^{2+}]_i$ of 0, 0.31, 1.2, 3.6, 7.2, 28, 127 μM and 10 mM were prepared using Ca^{2+} buffers EGTA (K_D = 150 nM at pH 7.2, total concentration 10 mM), *N*-hydroxyethylethylenediaminetriacetic acid (K_D = 3.6 μM, concentration 10 mM), or 2-ol-*N*, *N*′-tetraacetic acid (K_D = 81 μM, concentration 30 mM). Dissociation constants for the buffers are from Martell and Smith (1974–1989). Whole-cell recordings were made using each of the calibration solutions in the pipette, and the ratio of fluorescence emission (535 ± 25 nm) for 340 and 365 nm excitation were recorded after allowing 2 min for the pipette solution to diffuse into the cell. Three to five recordings were made for each calibration solution. The following equation was fit to the eight measured ratio values (R) to find the five unknown parameters (Voets, 2000):

$$R = R_0 + R_1\frac{[Ca^{2+}]_i}{[Ca^{2+}]_i + K_1} + R_2\frac{[Ca^{2+}]_i}{[Ca^{2+}]_i + K_2}.$$

Inversion of the equation was used to calculate $[Ca^{2+}]_i$ from the ratio *R* measured in caged Ca^{2+} experiments.

Electrophysiology and Photometry

Most experiments were performed at room temperature (~22°C) with the exception of the experiments depicted by the squares in Fig. 2. In these experiments, cells were warmed to 30–32°C by perfusing warmed bath solution. The temperature of the cells was confirmed by placing a small thermistor in the middle of the recording chamber.

Whole-cell patch-clamp measurements were performed using an EPC-9 patch-clamp amplifier and PULSE acquisition software (HEKA). Pipettes (2–4 MΩ) were pulled from Kimax glass capillaries, coated with dental wax at their tips, and fire polished. The pipette potential was held at a dc value of −70 mV except during membrane depolarization. Capacitance measurements were performed using the "sine + dc" software lock-in amplifier method implemented in PULSE software (Pusch and Neher, 1988; Gillis, 2000). The assumed reversal potential was 0 mV and the sinusoid had an amplitude of 25 mV and a frequency of 1.5 kHz.

A monochromator (Polychrome 4, TILL/ASI) coupled to the epifluorescence port of an Olympus IX-50 microscope with a fiber-optic cable excited the Ca^{2+} indicators at 340 and 365 nm. A two-port condensor (TILL/ASI) combined the monochromator excitation path with that of a flash lamp (TILL/ASI). A 40X 1.15 NA water immersion lens (U-APO; Olympus) focused the excitation light and collected fluorescent light. The fluorescent light (535 ± 25 nm) was measured using a photodiode mounted in a viewfinder (TILL/ASI).

Carbon Fiber Amperometry

Amperometric measurements were performed with carbon-fiber electrodes purchased from ALA, Inc. The tip of the carbon-fiber electrode was positioned to just touch the surface of a cell using a micromanipulator (PCS-5000; Burleigh). The amperometric current (I_{AMP}) generated by oxidation of 5-HT was measured using a patch-clamp amplifier (EPC-9; HEKA) while holding the potential of the carbon-fiber electrode at +700 mV. INS-1 cells were incubated in media containing 0.6 mM 5-HT and 0.6 mM 5-hydroxytryptophan for 5–10 h before initiating amperometric measurements (Smith et al., 1995; Zhou and Misler, 1996). The amperometric signal was filtered at 200 Hz and sampled at 1 kHz.

Data analysis and curve fitting were performed using Igor software (Wavemetrics). Analysis of amperometric spikes was performed using software described in Segura et al. (2000). Results and histograms are expressed as mean ± SEM. Statistical comparisons were performed using Student's *t* test. * denotes $P < 0.05$, whereas ** denotes $P < 0.01$.

RESULTS

Photoelevation of $[Ca^{2+}]$ into the Low Micromolar Range Results in a Small, Rapid Burst of Exocytosis

We introduced caged Ca^{2+} (0.5–1 mM nitrophenyl-EGTA loaded ~80% with $CaCl_2$) into INS-1 cells through the patch pipette during whole-cell recording. A combination of a high affinity Ca^{2+} indicator (bis-

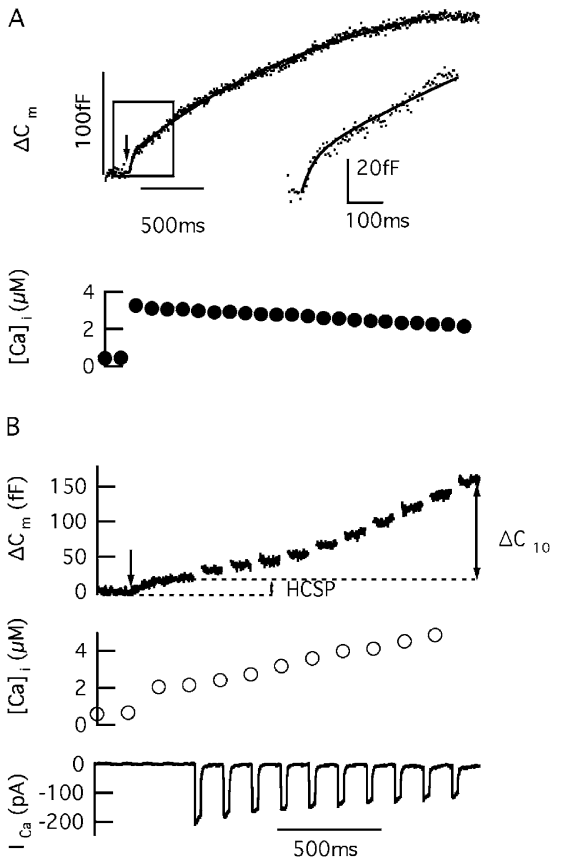

FIGURE 1. Photorelease of caged Ca^{2+} to low μM values in INS-1 cells results in a small burst of exocytosis we ascribe to release of an HCSP of granules. (A) Flash photoelevation of $[Ca^{2+}]_i$ to 3.3 μM (arrow) results in a capacitance increase (ΔC_m) with two kinetic components. The inset corresponds to the interval delineated by the box. The solid line indicates a double-exponential fit to the data with values indicated in the text. (B) Sample experiment following a protocol where flash photoelevation of $[Ca^{2+}]_i$ to release the HCSP is followed by a train of depolarizing pulses to release granules from the RRP. ΔC_{10} is defined as the change in C_m elicited by 10 depolarizing pulses, 30 ms in duration, from −70 to +20 mV.

fura-2) and a lower affinity indicator (fura-2FF) were also included in the pipette solution to allow ratiometric measurement of $[Ca^{2+}]_i$ over a wide concentration range (Voets, 2000). Fig. 1 A depicts a typical experiment where flash photolysis of the cage elevates $[Ca^{2+}]_i$ from a baseline value of 450 nM to 3.3 μM and leads to a rise in membrane capacitance (ΔC_m) of ~150 fF over several seconds that presumably reflects an increase in membrane surface area due to exocytosis. Note that the rate of exocytosis (dC/dt) declines despite the maintained elevation of $[Ca^{2+}]_i$. The most common explanation given for transient exocytosis with a maintained Ca^{2+} stimulus is depletion of one or more discrete pools of secretory vesicles. Closer inspection of Fig. 1 A reveals that there are at least two kinetic phases of exocytosis: a small, rapid burst followed by a larger, but slower phase. Fitting a sum of two exponentials to the ΔC_m trace reveals that the rapid phase has an amplitude of 18 fF and a time constant of 33 ms, whereas the slower component has an amplitude of 181 fF and is released with a time constant of 1.75 s. We do not know with certainty the unitary increase in capacitance that results from the fusion of an individual granule in INS-1 cells. However, if we assume that granules in INS-1 cells contribute about the same amount of membrane as those in mouse β cells (1.7 fF/granule; Ammala et al., 1993b) then the fast kinetic phase corresponds to exocytosis of ~10 granules, whereas ~100 granules are released during the slower phase.

The slower kinetic phase has an amplitude and kinetic rate similar to that previously reported for exocytosis from the RRP in β cells (Takahashi et al., 1997; Barg et al., 2001). The faster component has not previously been identified as a distinct phase of exocytosis in β cells, presumably because its small amplitude makes it easy to be overlooked. We have reported a similar kinetic phase of exocytosis from adrenal chromaffin cells that we attribute to release of an HCSP of granules.

Release from the HCSP is most prominent at low μM $[Ca^{2+}]_i$, however, release from the larger RRP is often too slow at these $[Ca^{2+}]_i$ values to be reliably measured. Fig. 1 B depicts a "hybrid stimulus" protocol we developed to estimate the size of the HCSP and RRP in a single sweep. We first use flash photolysis of caged Ca^{2+} to release the HCSP followed by 10 depolarizing pulses (30 ms in duration to +20 mV) to release most or all of the RRP. In the example of Fig. 1 B, the HCSP is ~19 fF, whereas the increase in C_m after 10 depolarizing pulses (ΔC_{10}) is ~142 fF, similar in size to the RRP defined from caged Ca^{2+} experiments (Fig. 1 A and Fig. 2). In the following experiments, we will use ΔC_{10} as a crude indicator of the size of the RRP, but it is not necessarily a direct measure because clear exhaustion of a releasable pool (i.e., smaller jumps in C_m for late pulses in the pulse train) is not always evident, perhaps because the RRP is being refilled during the train.

Dependence of the Kinetics of Release on $[Ca^{2+}]_i$ and Temperature

Fig. 2 presents a plot of the amplitude and rate constant (inverse time constant) of exponential fits to the ΔC_m time course as a function of $[Ca^{2+}]_i$ measured after the flash. Note that the rates, but not the amplitudes, of the kinetic phases of exocytosis depend on $[Ca^{2+}]_i$ after the flash. This observation is consistent with the hypothesis that the two kinetic phases of exocytosis correspond to depletion of two discrete pools of granules. We define the small pool underlying the faster kinetic phase as the HCSP (Fig. 2, circles and squares), whereas the slower phase is due to release from the previously described RRP (Fig. 2, triangles).

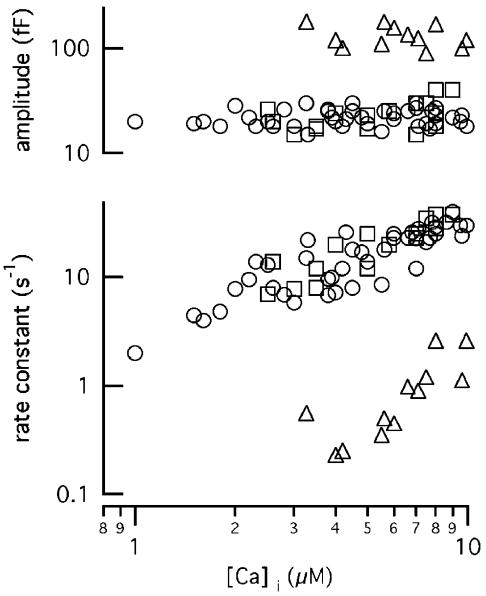

FIGURE 2. Dependence of the kinetics of exocytosis on $[Ca^{2+}]_i$ and temperature. The amplitudes and rate constants of exponential fits to ΔC_m are plotted versus the $[Ca^{2+}]_i$ level achieved upon flash photolysis of caged Ca^{2+}. Triangles are from the slower of double-exponential fits and presumably reflect release from the RRP. Circles and squares represent the fastest exponential component of fits and are interpreted as release from the HCSP. Circles represent experiments performed at room temperature (~22°C), whereas squares represent data from recording made between 30°C and 32°C. All experiments were performed with 10 mM glucose in the bath.

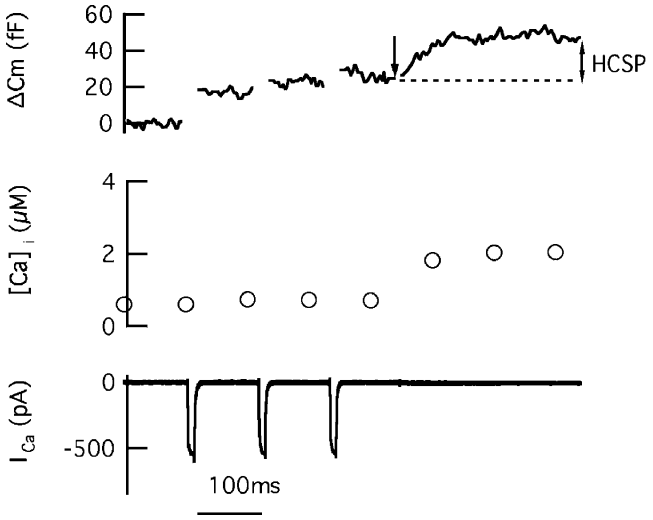

FIGURE 3. The HCSP is not exhausted with brief membrane depolarization. Sample experiment where three depolarizing pulses, 10 ms in duration, to +20 mV are applied to release granules located near Ca^{2+} channels (the IRP). This is quickly followed by flash photoelevation of $[Ca^{2+}]_i$ to 1.8 μM (arrow) to release the HCSP. Similar results were seen in seven other cells.

The size and $[Ca^{2+}]_i$-dependent rate constant of release of the RRP are similar to values previously reported in β cells. For example, rate constants for a $[Ca^{2+}]_i$ value of 10 μM are ~0.64 s^{-1} in Barg et al. (2001), ~1.0 s^{-1} in Takahashi et al. (1997), and ~10 s^{-1} in Wan et al. (2004). Note in Fig. 2 that the rate of release from the HCSP is an approximately linear function of $[Ca^{2+}]_i$, whereas release from the RRP is more steeply dependent on $[Ca^{2+}]_i$. The rate constant of exocytosis from the RRP has previously been shown to depend on $[Ca^{2+}]_i$ raised to the 3rd–5th power in β cells (Takahashi et al., 1999; Barg et al., 2001), chromaffin cells (Heinemann et al., 1994; Voets, 2000), melanotrophs (Thomas et al., 1993), hair cells (Beutner et al., 2001), and neurons (Heidelberger et al., 1994; Bollmann et al., 2000; Schneggenburger and Neher, 2000). A shallow dependence of the rate of release from the HCSP on $[Ca^{2+}]_i$ is also observed in chromaffin cells (Yang et al., 2002) and in rat β cells (Wan et al., 2004). Nevertheless, the release rate from the HCSP may drop steeply for $[Ca^{2+}]_i < 1$ μM, because the baseline rate of exocytosis preceding photoelevation of $[Ca^{2+}]_i$ is very low (unpublished data).

We performed most experiments at room temperature (~22°C), which is sufficient to support exocytosis from most neuroendocrine cells (e.g., Thomas et al., 1993; Dinkelacker et al., 2000), whereas temperatures >~28°C are usually thought to be necessary to support exocytosis from primary β cells (e.g., Atwater et al., 1984; Gillis and Misler, 1992; Renstrom et al., 1996). We performed a set of experiments to see if the size or time course of release of the HCSP is affected by raising the temperature to 30–32°C. The squares in Fig. 2 represent exponential fits to data obtained at this higher temperature range, whereas the circles are from experiments performed at room temperature. These data demonstrate that neither the number of granules in the HCSP nor the Ca^{2+}-dependent rate of release are steeply dependent on temperature in INS-1 cells. We also find that depolarization-evoked ΔC_m responses in INS-1 cells are not highly sensitive to temperature over this range (unpublished data).

The HCSP Is Not Exhausted with Brief Membrane Depolarization

The first vesicles released during membrane depolarization are generally thought to be located nearby Ca^{2+} channels and have been termed the immediately releasable pool (IRP; Horrigan and Bookman, 1994; Barg et al., 2001). We designed an experiment to test if the HCSP is released in response to brief membrane depolarization due to its high sensitivity to Ca^{2+}. Fig. 3 presents a sample experiment, representative of responses from eight cells, where photoelevation of $[Ca^{2+}]_i$ to 1.8 μM is still able to elicit release from the HCSP following three brief (10 ms) depolarizing pulses to deplete

the IRP. Note that the ΔC_m responses to the second and third pulses are substantially smaller than the response to the first pulse, demonstrating that the first pulse exhausted the IRP and that it takes substantially longer than 200 ms for the IRP to refill. Since an HCSP is still present after exhaustion of the IRP, the HCSP must be a distinct population of vesicles from the IRP, and a substantial fraction of the vesicles in the HCSP do not appear to be located particularly close to Ca^{2+} channels.

The Size of the HCSP Is Modulated by Glucose, PKA, and PKC

Glucose stimulates insulin release through membrane depolarization triggered by closure of K^+(ATP) channels, but also has one or more roles in "priming" insulin granules for exocytosis. Fig. 4 A presents sample experiments following the protocol of Fig. 1 B to investigate modulation of the HCSP size with preincubation of cells in various concentrations of glucose. The HCSP is very small or absent in cells incubated in 2.6 mM glucose but is maximally stimulated at 10 mM glucose. The ΔC_{10} response also was sensitive to glucose and roughly doubled in size between 2.6 and 10 mM glucose, whereas the Ca^{2+} current and total Ca^{2+} influx (Q_{Ca}) are unaffected by the sugar. Results summarized in Fig. 4 B suggest that the size of the HCSP may be more sensitive to glucose than the RRP.

The second messenger cAMP stimulates exocytosis from β cells by increasing the amount of release for a given amount of Ca^{2+} influx (Jones et al., 1986; Ammala et al., 1993a; Gillis and Misler, 1993; Renstrom et al., 1997; Eliasson et al., 2003). Fig. 5 A depicts sample experiments demonstrating that including cAMP (0.2–1 mM) in the pipette solution increases the size of the HCSP and the ΔC_{10} response. The enhancement of exocytosis by cAMP can be completely blocked by including PKI (0.5 mM), a peptide inhibitor of PKA, in the pipette. Including a membrane permeant analogue of cAMP (CPT-cAMP, 100 μM) in the bath solution also increases the size of the HCSP and the ΔC_{10} response, and this enhancement is completely blocked by the PKA inhibitor Rp-cAMP (0.5 mM, Fig. 5 B). The results summarized in Fig. 5 B suggest that the HCSP and RRP are both increased approximately twofold by cAMP and that this effect appears to be completely attributable to activation of PKA in INS-1 cells.

The rate constant and amplitude of release from the HCSP with cAMP in the pipette are depicted with filled circles in Fig. 6. The control values from Fig. 2 (open circles and triangles) are also included in Fig. 6 for comparison. These data demonstrate that cAMP does not affect the kinetics or intrinsic Ca^{2+} sensitivity of release from the HCSP.

Activation of PKC by phorbol esters also potently increases the amount of exocytosis for a given influx of

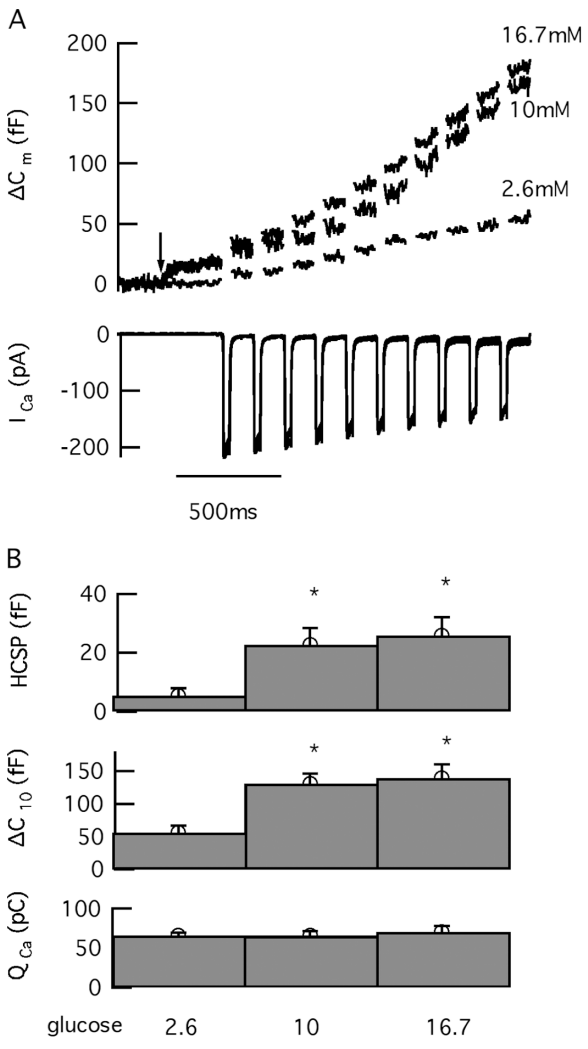

FIGURE 4. Glucose increases the size of the RRP and the HCSP but has little effect on the Ca^{2+} current (I_{Ca}). (A) Sample experiments following the protocol from Fig. 1 B executed from cells incubated for at least 10 min in the indicated concentration of glucose. (B) Summary data in paired experiments with each condition representing 20 cells. Q_{Ca} refers to the integral of Ca^{2+} influx during the depolarizing pulses.

Ca^{2+} in β cells (Ammala et al., 1994). In chromaffin cells, activation of PKC increases the size of the HCSP approximately sixfold while increasing the RRP by two to threefold (Gillis et al., 1996; Yang et al., 2002). Fig. 7 demonstrates that activation of PKC with bath application of PMA (100 nM) increases the HCSP and the ΔC_{10} response by two to threefold in INS-1 cells. This enhancement can be completely blocked by bisindoylymaleimide I (1 μM), a selective inhibitor of PKC.

The rate constant and amplitude of the HCSP obtained from cells incubated in PMA are plotted as asterisks in Fig. 6. Thus PMA, like cAMP, does not affect the time course and Ca^{2+} sensitivity of release from the HCSP. A similar affect of PMA on the amplitude, but not the time course, of release from the HCSP has pre-

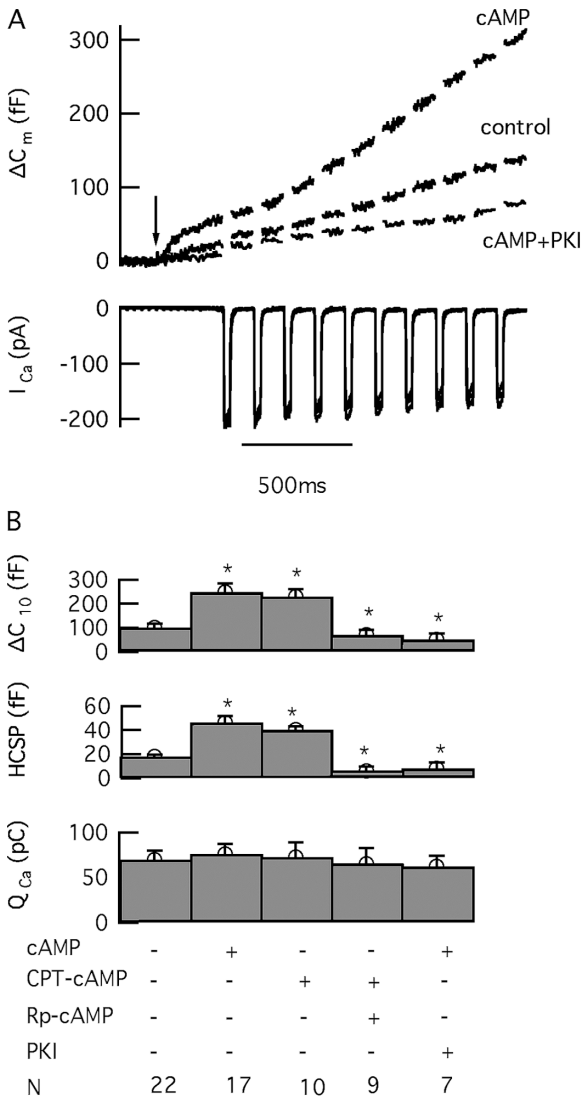

FIGURE 5. cAMP acting through PKA increases the size of the RRP and the HCSP. (A) Sample experiments following the protocol from Fig. 1 B under control conditions or with 100 μM cAMP in the pipette or with cAMP plus PKI (0.5 mM) in the pipette. (B) Summary data with paired cells. Membrane permeant cAMP analogue (8-CPT-cAMP, 100 μM) and PKA inhibitor (Rp-cAMP, 0.5 mM) were included in the bath solution at the indicated concentration. All experiments were performed with 10 mM glucose in the bath.

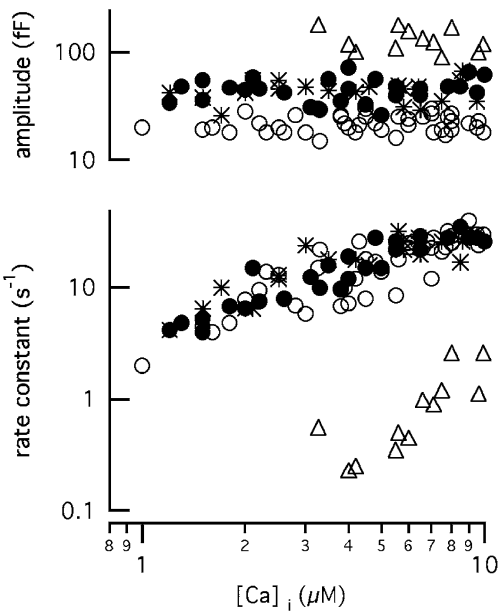

FIGURE 6. The amplitude, but not the Ca^{2+}-dependent rate of exocytosis, of the HCSP is modulated by PKA and PKC. The amplitude and rate constant obtained from exponential fits to the initial ΔC_m response (the HCSP) were obtained from recordings made with either 100 μM cAMP in the pipette (filled circles) or with 100 nM PMA in the bath (asterisks). Control data for the HCSP (open circles) and RRP (triangles) are the same as depicted in Fig. 2 and are included here for comparison. All experiments included 10 mM glucose in the bath and were made at room temperature.

viously been reported in chromaffin cells (Yang et al., 2002).

We tested combinations of glucose, cAMP, and PMA in paired experiments to determine if the enhancement of exocytosis by these agents involves common mechanisms. Fig. 8 (A and B) demonstrates that preincubation of cells in 10 mM glucose results in larger granule pool sizes than preincubation in 2 mM glucose even in the presence of high concentrations of cAMP and PMA, thus it is likely that glucose enhances exocytosis by mechanisms independent of the PKA and PKC stimulatory pathways. In contrast, Fig. 8 C demonstrates that the actions of PKA and PKC on enhancing pool sizes are not additive and therefore may involve a common mechanism.

Amperometric Measurement of 5-HT Release Suggests that the HCSP and the RRP Are Composed of Morphologically Similar Granules

Carbon-fiber amperometry has proven to be a powerful tool to measure the contents and release kinetics of individual catecholamine-containing vesicles. The technique can also be used to measure release of 5-HT from β cells preincubated with 5-HT and a precursor (Smith et al., 1995; Zhou and Misler, 1996). 5-HT is accumulated in insulin-containing granules, and release of this electro-oxidizable indolamine has been shown to be an accurate and specific marker of insulin granule exocytosis in β cells (Aspinwall et al., 1999).

Fig. 9 A depicts a sample trace where flash photolysis elevates $[Ca^{2+}]_i$ to 3.7 μM, leading to release of the HCSP. The flash is followed 1 s later by a train of depolarizing pulses to release granules from the RRP. Spikes of oxidative current are recorded during both phases of release with each spike reporting release of 5-HT from an individual granule. Significant cell-to-cell vari-

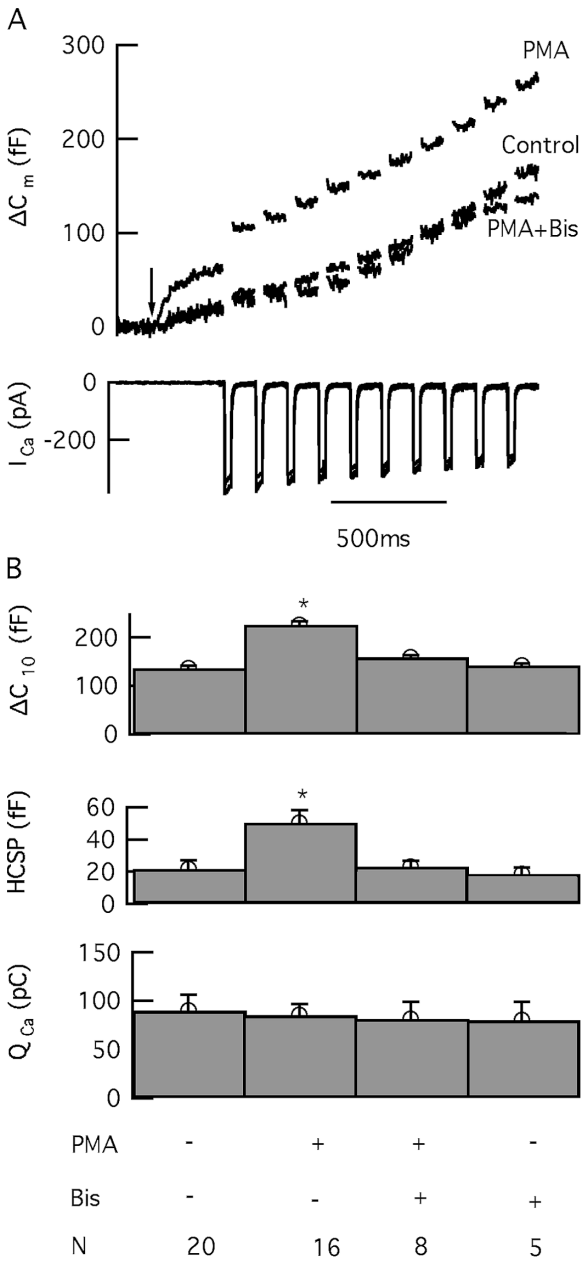

FIGURE 7. The phorbol ester PMA increases the size of the RRP and the HCSP by activating PKC. (A) Sample experiments under control conditions or with 100 nM PMA in the bath solution, or PMA plus the PKC inhibitor bisindoylymaleimide I (Bis, 1 μM) in the bath. (B) Summary data in paired experiments. All experiments were performed with 10 mM glucose in the bath.

ability of responses occurs because only those granule fusion events that occur in the ~10–15% of the membrane that is directly adjacent to the carbon-fiber microelectrode are captured. Fig. 9 B presents the averaged response from 22 sweeps taken from 17 cells. The amperometric current is integrated to give an indicator of cumulative release (Q_{amp}) and is scaled to match the maximal ΔC_m signal. Note that the ratio of Q_{amp} to ΔC_m is similar for release of the HCSP and the RRP, suggesting that the granules in these two pools have a similar diameter (see DISCUSSION). The good correspondence between the time course of Q_{amp} and ΔC_m also demonstrates that endocytosis does not greatly affect the kinetics of ΔC_m under our recording conditions.

Fig. 9 C is a cumulative histogram comparing the charge of individual spikes released from the HCSP (dashed line, $n = 78$) and the RRP (solid line, $n = 153$) from 17 cells. Q_{amp} is 0.11 ± 0.02 pC for HCSP spikes and 0.16 ± 0.07 pC for RRP spikes. Fig. 9 D presents a cumulative histogram of $t_{1/2}$, defined as the time interval between the rising and falling phase of a spike where I_{amp} assumes the half-maximal value. The value of $t_{1/2}$ is 4.16 ± 0.61 ms for HCSP spikes versus 3.84 ± 0.42 ms for RRP spikes. Thus the quantal content and the time course of release of 5-HT from granules is similar for the RRP and the HCSP, and it is therefore unlikely that vesicles in the two pools differ in gross morphology.

DISCUSSION

We describe a small (~14 granule), but relatively rapid, burst of exocytosis in INS-1 cells that is prominent when $[Ca^{2+}]_i$ is rapidly elevated into the low μM range. We attribute this burst of exocytosis to release of an HCSP of vesicles with characteristics that are very similar to what we previously described in adrenal chromaffin cells. A companion article in this issue (Wan et al., 2004) reports an HCSP in rat β cells with a size nearly identical to what we observe but with somewhat higher sensitivity to $[Ca^{2+}]_i$. Exocytosis with a similar sensitivity to Ca^{2+} has also recently been reported in rod photoreceptors (Thoreson et al., 2004) and in pituitary gonadotropes (Zhu et al., 2002).

Regulation of the HCSP by Second Messengers and Temperature

The size, but not the rate constant of release, of the HCSP is sensitive to cAMP and the phorbol ester PMA (Fig. 6; also see Wan et al., 2004). The enhancement of pool size by PMA can be completely blocked with bisindolylmaleimide I (Fig. 7) and other specific PKC blockers (Wan et al., 2004), supporting the hypothesis that phorbol esters enhance exocytosis from neuroendocrine cells by activating PKC. In contrast, the enhancement of release from hippocampal nerve terminals by phorbol esters is reported to be mediated by munc-13 (Rhee et al., 2002). We find that PKI and Rp-cAMP, specific inhibitors of PKA, can completely block the ability of cAMP to increase the size of the HCSP and RRP. Similarly, Wan et al. (2004) report a complete block of the forskolin-induced enhancement of HCSP and RRP pool sizes by Rp-cAMP. These findings are surprising

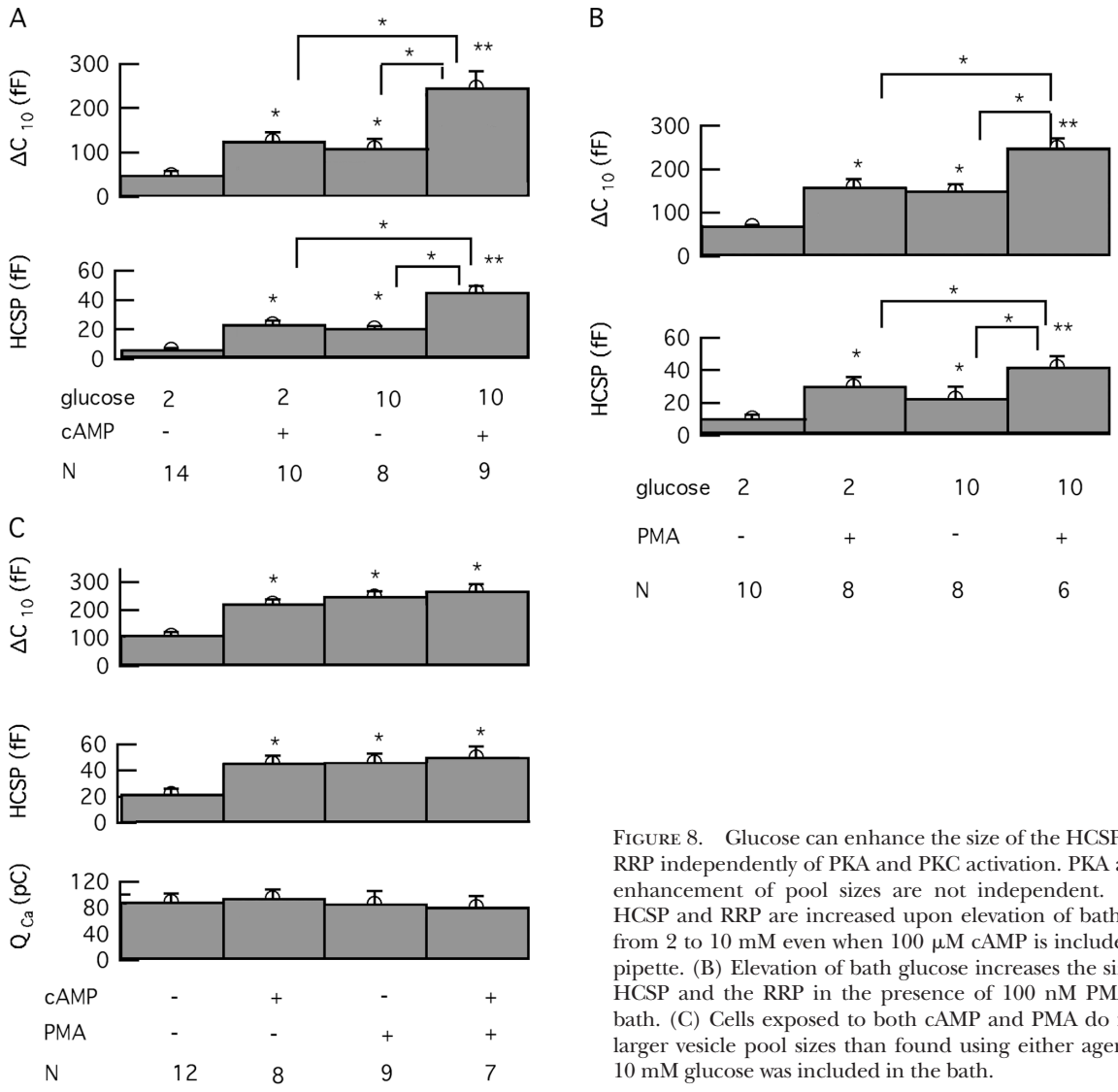

FIGURE 8. Glucose can enhance the size of the HCSP and the RRP independently of PKA and PKC activation. PKA and PKC enhancement of pool sizes are not independent. (A) The HCSP and RRP are increased upon elevation of bath glucose from 2 to 10 mM even when 100 μM cAMP is included in the pipette. (B) Elevation of bath glucose increases the size of the HCSP and the RRP in the presence of 100 nM PMA in the bath. (C) Cells exposed to both cAMP and PMA do not have larger vesicle pool sizes than found using either agent alone. 10 mM glucose was included in the bath.

because previous reports describe only a partial block of the cAMP-induced enhancement of depolarization-evoked exocytosis by PKA inhibitors in mouse β cells and INS-1 cells (Renstrom et al., 1997; Rosengren et al., 2002). This has led to the hypothesis that cAMP enhances exocytosis through a PKA-independent pathway such as cAMP-GEFII (Eliasson et al., 2003). It should be noted that we use a relatively high concentration of PKI in the pipette (0.5–1 mM) because, e.g., high concentrations of PKI are necessary to rapidly and completely block PKA-dependent activation of the CFTR Cl^- channel during whole-cell recordings in cardiac myocytes (Hwang et al., 1993). The effects of saturating doses of cAMP and PMA on enhancing granule pool sizes do not appear to be additive (Fig. 8 C), therefore PKA and PKC may converge on a common mechanism of action.

Activation of PKA or PKC increases the size of both the HCSP and the RRP by approximately twofold (Figs. 5 and 7), thus PKA and PKC do not appear to change the fraction of releasable granules that are in a highly Ca^{2+}-sensitive state in INS-1 cells. In contrast, PKC increases the fraction of granules in the HCSP in chromaffin cells (Yang et al., 2002), and both PKC and PKA increase the fraction of granules in the HCSP in rat β cells (Wan et al., 2004). Our data suggest that the fraction of granules in the highly Ca^{2+}-sensitive state may be higher when glucose is elevated in INS-1 cells (Fig. 4), but further study is necessary to confirm this trend. If so, then this would provide a mechanism for glucose to increase the sensitivity of insulin granule exocytosis to modest increases in $[Ca^{2+}]_i$. Further studies of the modulation of HCSP and RRP pool sizes could benefit from using the perforated patch configuration to maintain a more physiological intracellular milieu (Horn and Marty, 1988; Gillis et al., 1991).

Our data show that the size and release kinetics of the HCSP (Fig. 2) and RRP (not depicted) are not highly temperature sensitive in INS-1 cells over a range

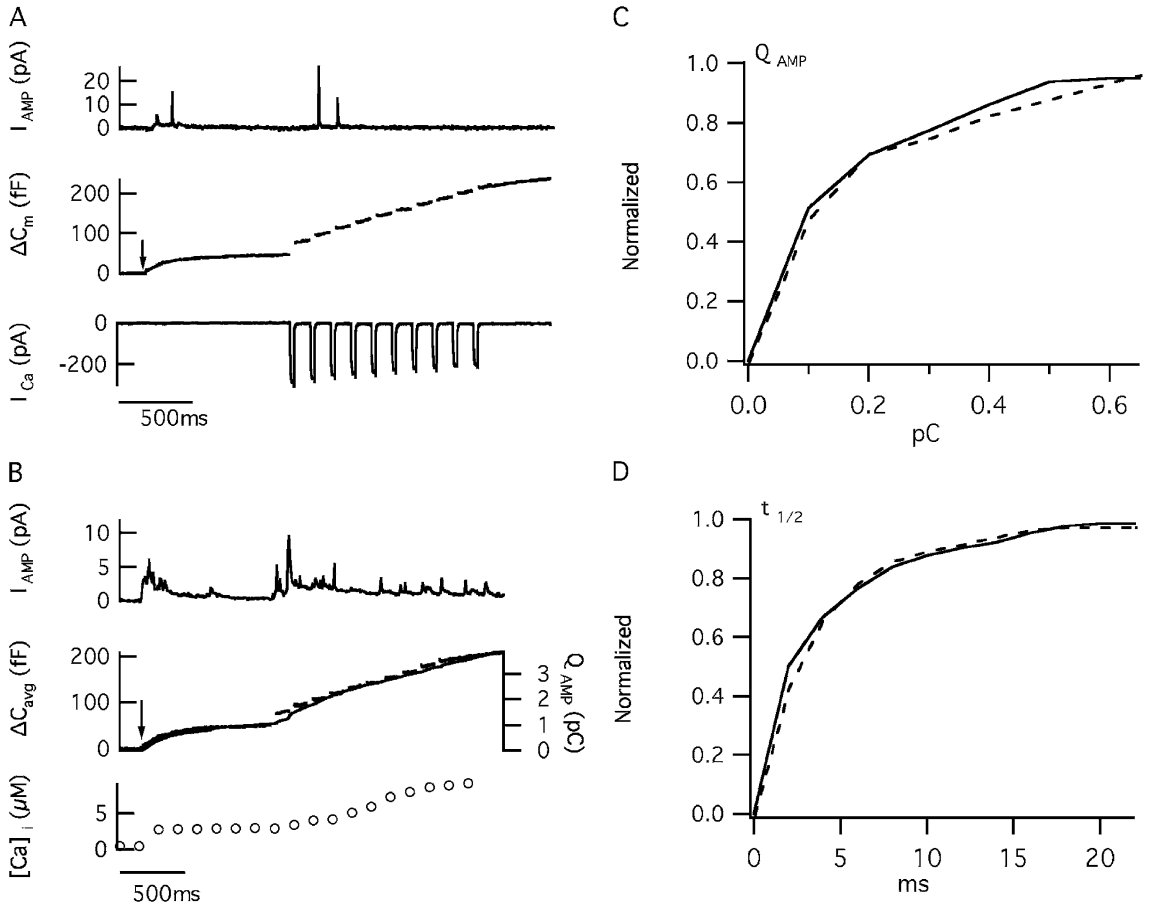

FIGURE 9. Granules in the HCSP have a similar size and release kinetics as granules in the RRP. (A) Sample experiment where a carbon-fiber electrode measures the amperometric current (I_{AMP}) resulting from oxidation of 5-HT released from insulin granules. Amperometric spikes occurring shortly after photoelevation of $[Ca2+]_i$ to the low μM range are assumed to be from the HCSP, whereas spikes that follow membrane depolarization are assumed to be from the RRP. (B) Averaged response from 22 sweeps taken from 17 cells. Q_{AMP}, the integral of I_{AMP}, is an indicator of cumulative release and is scaled to match the maximal ΔC_m signal. We only included sweeps in the average that contained at least one spike to ensure that the carbon-fiber electrode was responsive. The most responsive traces had 10 spikes (13% of total) in the HCSP phase and 17 spikes (11% of total) in the RRP phase. The mean number of spikes per sweep included in the average was 3.5 for the HCSP phase and 7.0 for the RRP phase. (C) Cumulative histogram comparing the charge of individual spikes released from the HCSP (dashed line, $n = 78$) and the RRP (solid line, $n = 153$) from 17 cells. (D) Cumulative histogram of $t_{1/2}$ from the same spikes analyzed in part C.

(22–32°C) where the size of the depolarization-evoked ΔC_m responses change many fold in primary β cells (Gillis and Misler, 1992; Renstrom et al., 1996). This finding likely indicates a difference in the temperature sensitivity of insulin secretion between INS-1 cells and primary β cells (but see Sheu et al., 2003). Another intriguing possibility is that the high basal (preflash) $[Ca^{2+}]_i$ in our experiments (0.5–0.7 μM) overcomes a temperature-sensitive step in vesicle priming.

How Does Glucose Increase the Size of Granule Pools?

Preincubation of INS-1 cells in glucose increases the size of the HCSP and the RRP (Fig. 4; also see Rosengren et al., 2002). Glucose is often thought to influence insulin secretion by increasing the ATP concentration or the ATP/ADP ratio in the cell. However, during whole-cell recording, the ATP concentration is clamped to the value in the pipette solution (2 mM) following a brief interval of dialysis. Thus, the enhancement of vesicle pool size must either be a long-lived effect of previous elevation of ATP or some other mechanism that is resistant to whole-cell dialysis. Preincubation of cells in 10 mM glucose results in larger granule pool sizes than incubation in 2 mM glucose even when combined with a high concentration of cAMP (1 mM in the pipette) or PMA (100 nM in the bath). Thus glucose does not work exclusively by activating PKA or PKC to increase granule pool sizes. Further experiments are needed to determine if the glucose effect we observe is mediated by membrane depolarization and Ca^{2+} influx that occurs before the cells are voltage clamped for our recording.

The HCSP Is Likely to be Composed of Insulin-containing Granules

β cells contain small GABA-containing synaptic-like vesicles in addition to dense-core insulin-containing granules (Thomas-Reetz and De Camilli, 1994), so it is natural to question whether distinct kinetic phases of exocytosis measured as membrane capacitance changes correspond to release of morphologically distinct types of vesicles (Takahashi et al., 1997). However, it has recently been estimated that release of GABA-containing synaptic-like vesicles only contributes ~1% of the capacitance signal in β cells (Braun et al., 2004). Our measurements of quantal 5-HT release using carbon-fiber microelectrodes supports the hypothesis that the HCSP and the "conventional" releasable pool (the RRP) consist of the same type of vesicle. Simultaneous measurement of insulin and 5-HT release with modified carbon fiber electrodes demonstrates that 5-HT is released exclusively from insulin-containing granules (Aspinwall et al., 1999). We find that the amount of 5-HT released from a single vesicle and oxidized on the surface of the carbon fiber (Q_{amp}) is similar for the two kinetic phases of exocytosis (Fig. 9 C). The time course of release of 5-HT from individual vesicles in the two pools also does not appreciably differ (Fig. 9 D). Since the single-granule Q_{amp} and the ratio of the cumulative ΔC_m to Q_{amp} are the same for the two pools (Fig. 9 B), the ΔC_m due to fusion of a single vesicle is likely to be the same for the HCSP and the RRP. The single-vesicle ΔC_m is proportional to the diameter squared, so vesicles in the HCSP have a similar size as vesicles in the RRP. Thus the HCSP does not appear to be a morphologically distinct type of vesicle, but rather a distinct granule "state." It seems likely that vesicles in the highly Ca^{2+}-sensitive state posses either a different Ca^{2+} sensor or a different conformation of Ca^{2+}-sensing proteins.

Physiological Role of HCSP in Insulin Secretion

The rate constant of exocytosis from the HCSP has a shallower dependence on $[Ca^{2+}]_i$ than the rate constant of release of the RRP (Fig. 2). Thus the rate of exocytosis from the HCSP dominates for $[Ca^{2+}]_i < \sim 10$ μM, but will actually be slower than the rate of release from the RRP at higher $[Ca^{2+}]_i$ levels. This suggests that the highly Ca^{2+}-sensitive triggering mechanism may have a higher affinity for Ca^{2+}, but a lower efficacy in triggering fast exocytosis. Thus, it would appear that the HCSP release mode is specialized for mediating slow exocytosis in response to modest elevations of $[Ca^{2+}]_i$. Our finding that the bulk of the HCSP is not released in response to brief depolarization (Fig. 3) suggests that many of the vesicles in the HCSP do not reside close to Ca^{2+} channels. Thus, the HCSP is likely to respond to global elevations of $[Ca^{2+}]_i$ that result from action potential trains or release of Ca^{2+} from internal stores by hormone agonists. The modulation of the HCSP by PKA and PKC may explain how a phorbol ester can stimulate insulin secretion at a subthreshold glucose concentration (Bozem et al., 1987) and how PKA and PKC can elicit exocytosis from β cells at substimulatory $[Ca^{2+}]_i$ values (Jones et al., 1985, 1986). In contrast, the RRP release mechanism is specialized for fast, synchronous release of granules that experience high $[Ca^{2+}]_i$ during action potentials due to their close proximity to Ca^{2+} channels.

We thank Prof. Claes Wollheim for providing the INS-1 cell line and Vanessa Melton for technical assistance. We also thank Miguel A. Brioso and Ricardo Borges (Universidad de La Laguna, Tenerife, Spain) for providing software support for analysis of amperometric spikes.

This work was supported by National Institutes of Health R01 NS40453 to K.D. Gillis.

Olaf S. Andersen served as editor.

Submitted: 27 April 2004
Accepted: 15 October 2004

REFERENCES

Ammala, C., F.M. Ashcroft, and P. Rorsman. 1993a. Calcium-independent potentiation of insulin release by cyclic AMP in single β-cells. *Nature.* 363:356–358.

Ammala, C., L. Eliasson, K. Bokvist, P.O. Berggren, R.E. Honkanen, A. Sjoholm, and P. Rorsman. 1994. Activation of protein kinases and inhibition of protein phosphatases play a central role in the regulation of exocytosis in mouse pancreatic β cells. *Proc. Natl. Acad. Sci. USA.* 91:4343–4347.

Ammala, C., L. Eliasson, K. Bokvist, O. Larsson, F.M. Ashcroft, and P. Rorsman. 1993b. Exocytosis elicited by action potentials and voltage-clamp calcium currents in individual mouse pancreatic B-cells. *J. Physiol.* 472:665–688.

Asfari, M., D. Janjic, P. Meda, G. Li, P.A. Halban, and C.B. Wollheim. 1992. Establishment of 2-mercaptoethanol-dependent differentiated insulin-secreting cell lines. *Endocrinology.* 130:167–178.

Aspinwall, C.A., L. Huang, J.R. Lakey, and R.T. Kennedy. 1999. Comparison of amperometric methods for detection of exocytosis from single pancreatic β-cells of different species. *Anal. Chem.* 71:5551–5556.

Atwater, I., A. Goncalves, A. Herchuelz, P. Lebrun, W.J. Malaisse, E. Rojas, and A. Scott. 1984. Cooling dissociates glucose-induced insulin release from electrical activity and cation fluxes in rodent pancreatic islets. *J. Physiol.* 348:615–627.

Barg, S., X. Ma, L. Eliasson, J. Galvanovskis, S.O. Gopel, S. Obermuller, J. Platzer, E. Renstrom, M. Trus, D. Atlas, et al. 2001. Fast exocytosis with few Ca^{2+} channels in insulin-secreting mouse pancreatic B cells. *Biophys. J.* 81:3308–3323.

Beutner, D., T. Voets, E. Neher, and T. Moser. 2001. Calcium dependence of exocytosis and endocytosis at the cochlear inner hair cell afferent synapse. *Neuron.* 29:681–690.

Bollmann, J.H., B. Sakmann, and J.G. Borst. 2000. Calcium sensitivity of glutamate release in a calyx-type terminal. *Science.* 289:953–957.

Bozem, M., M. Nenquin, and J.C. Henquin. 1987. The ionic, electrical, and secretory effects of protein kinase C activation in mouse pancreatic B-cells: studies with a phorbol ester. *Endocrinology.* 121:1025–1033.

Braun, M., A. Wendt, B. Birnir, J. Broman, L. Eliasson, J. Gal-

vanovskis, J. Gromada, H. Mulder, and P. Rorsman. 2004. Regulated exocytosis of GABA-containing synaptic-like microvesicles in pancreatic β-cells. *J. Gen. Physiol.* 123:191–204.

Dinkelacker, V., T. Voets, E. Neher, and T. Moser. 2000. The readily releasable pool of vesicles in chromaffin cells is replenished in a temperature-dependent manner and transiently overfills at 37°C. *J. Neurosci.* 20:8377–8383.

Eliasson, L., X. Ma, E. Renstrom, S. Barg, P.O. Berggren, J. Galvanovskis, J. Gromada, X. Jing, I. Lundquist, A. Salehi, et al. 2003. SUR1 regulates PKA-independent cAMP-induced granule priming in mouse pancreatic B-cells. *J. Gen. Physiol.* 121:181–197.

Eliasson, L., E. Renstrom, W.G. Ding, P. Proks, and P. Rorsman. 1997. Rapid ATP-dependent priming of secretory granules precedes Ca^{2+}-induced exocytosis in mouse pancreatic B-cells. *J. Physiol.* 503(Pt 2):399–412.

Ellis-Davies, G.C., and J.H. Kaplan. 1994. Nitrophenyl-EGTA, a photolabile chelator that selectively binds Ca^{2+} with high affinity and releases it rapidly upon photolysis. *Proc. Natl. Acad. Sci. USA*. 91: 187–191.

Gillis, K.D. 2000. Admittance-based measurement of membrane capacitance using the EPC-9 patch-clamp amplifier. *Pflugers Arch.* 439:655–664.

Gillis, K.D., and S. Misler. 1992. Single cell assay of exocytosis from pancreatic islet B cells. *Pflugers Arch.* 420:121–123.

Gillis, K.D., and S. Misler. 1993. Enhancers of cytosolic cAMP augment depolarization-induced exocytosis from pancreatic B-cells: evidence for effects distal to Ca^{2+} entry. *Pflugers Arch.* 424:195–197.

Gillis, K.D., R. Mössner, and E. Neher. 1996. Protein kinase C enhances exocytosis from chromaffin cells by increasing the size of the readily releasable pool of secretory granules. *Neuron.* 16: 1209–1220.

Gillis, K.D., R.Y. Pun, and S. Misler. 1991. Single cell assay of exocytosis from adrenal chromaffin cells using "perforated patch recording." *Pflugers Arch.* 418:611–613.

Heidelberger, R., C. Heinemann, E. Neher, and G. Matthews. 1994. Calcium dependence of the rate of exocytosis in a synaptic terminal. *Nature.* 371:513–515.

Heinemann, C., R.H. Chow, E. Neher, and R.S. Zucker. 1994. Kinetics of the secretory response in bovine chromaffin cells following flash photolysis of caged Ca^{2+}. *Biophys. J.* 67:2546–2557.

Horn, R., and A. Marty. 1988. Muscarinic activation of ionic currents measured by a new whole-cell recording method. *J. Gen. Physiol.* 92:145–159.

Horrigan, F., and R. Bookman. 1994. Releasable pools and the kinetics of exocytosis in adrenal chromaffin cells. *Neuron.* 13:1119–1129.

Hwang, T.C., M. Horie, and D.C. Gadsby. 1993. Functionally distinct phospho-forms underlie incremental activation of protein kinase–regulated Cl^- conductance in mammalian heart. *J. Gen. Physiol.* 101:629–650.

Jones, P.M., J.M. Fyles, and S.L. Howell. 1986. Regulation of insulin secretion by cAMP in rat islets of Langerhans permeabilised by high-voltage discharge. *FEBS Lett.* 205:205–209.

Jones, P.M., and S.J. Persaud. 1998. Protein kinases, protein phosphorylation, and the regulation of insulin secretion from pancreatic β-cells. *Endocr. Rev.* 19:429–461.

Jones, P.M., J. Stutchfield, and S.L. Howell. 1985. Effects of Ca^{2+} and a phorbol ester on insulin secretion from islets of Langerhans permeabilised by high-voltage discharge. *FEBS Lett.* 191: 102–106.

Martell, A.E., and R.H. Smith. 1974–1989. Critical Stability Constants. Vol. 1–6. Plenum Press, New York.

Pusch, M., and E. Neher. 1988. Rates of diffusional exchange between small cells and a measuring patch pipette. *Pflugers Arch.* 411:204–211.

Renstrom, E., L. Eliasson, K. Bokvist, and P. Rorsman. 1996. Cooling inhibits exocytosis in single mouse pancreatic B-cells by suppression of granule mobilization. *J. Physiol.* 494:41–52.

Renstrom, E., L. Eliasson, and P. Rorsman. 1997. Protein kinase A-dependent and -independent stimulation of exocytosis by cAMP in mouse pancreatic B-cells. *J. Physiol.* 502:105–118.

Rhee, J.S., A. Betz, S. Pyott, K. Reim, F. Varoqueaux, I. Augustin, D. Hesse, T.C. Sudhof, M. Takahashi, C. Rosenmund, and N. Brose. 2002. β phorbol ester- and diacylglycerol-induced augmentation of transmitter release is mediated by Munc13s and not by PKCs. *Cell.* 108:121–133.

Rosengren, A., K. Filipsson, X.J. Jing, M.K. Reimer, and E. Renstrom. 2002. Glucose dependence of insulinotropic actions of pituitary adenylate cyclase-activating polypeptide in insulin-secreting INS-1 cells. *Pflugers Arch.* 444:556–567.

Schneggenburger, R., and E. Neher. 2000. Intracellular calcium dependence of transmitter release rates at a fast central synapse. *Nature.* 406:889–893.

Segura, F., M.A. Brioso, J.F. Gomez, J.D. Machado, and R. Borges. 2000. Automatic analysis for amperometrical recordings of exocytosis. *J. Neurosci. Methods.* 103:151–156.

Sheu, L., E.A. Pasyk, J. Ji, X. Huang, X. Gao, F. Varoqueaux, N. Brose, and H.Y. Gaisano. 2003. Regulation of insulin exocytosis by Munc13-1. *J. Biol. Chem.* 278:27556–27563.

Smith, P.A., M.R. Duchen, and F.M. Ashcroft. 1995. A fluorimetric and amperometric study of calcium and secretion in isolated mouse pancreatic β-cells. *Pflugers Arch.* 430:808–818.

Takahashi, N., T. Kadowaki, Y. Yazaki, G.C. Ellis-Davies, Y. Miyashita, and H. Kasai. 1999. Post-priming actions of ATP on Ca^{2+}-dependent exocytosis in pancreatic β cells. *Proc. Natl. Acad. Sci. USA*. 96: 760–765.

Takahashi, N., T. Kadowaki, Y. Yazaki, Y. Miyashita, and H. Kasai. 1997. Multiple exocytotic pathways in pancreatic β cells. *J. Cell Biol.* 138:55–64.

Thomas, P., J.G. Wong, A.K. Lee, and W. Almers. 1993. A low affinity Ca^{2+} receptor controls the final steps in peptide secretion from pituitary melanotrophs. *Neuron.* 11:93–104.

Thomas-Reetz, A.C., and P. De Camilli. 1994. A role for synaptic vesicles in non-neuronal cells: clues from pancreatic β cells and from chromaffin cells. *FASEB J.* 8:209–216.

Thoreson, W.B., K. Rabl, E. Townes-Anderson, and R. Heidelberger. 2004. A highly Ca^{2+}-sensitive pool of vesicles contributes to linearity at the rod photoreceptor ribbon synapse. *Neuron.* 42: 595–605.

Voets, T. 2000. Dissection of three Ca^{2+}-dependent steps leading to secretion in chromaffin cells from mouse adrenal slices. *Neuron.* 28:537–545.

Wan, Q.-F., H. Yang, X. Lou, J. Ding, and T. Xu. 2004. Protein kinase activation increases insulin secretion by sensitizing the secretory machinery to Ca^{2+}. *J. Gen. Physiol.* 124:653–662.

Wiser, O., M. Trus, A. Hernandez, E. Renstrom, S. Barg, P. Rorsman, and D. Atlas. 1999. The voltage sensitive Lc-type Ca^{2+} channel is functionally coupled to the exocytotic machinery. *Proc. Natl. Acad. Sci. USA*. 96:248–253.

Yang, Y., S. Udayasankar, J. Dunning, P. Chen, and K.D. Gillis. 2002. A highly Ca^{2+}-sensitive pool of vesicles is regulated by protein kinase C in adrenal chromaffin cells. *Proc. Natl. Acad. Sci. USA*. 99: 17060–17065.

Zhou, Z., and S. Misler. 1996. Amperometric detection of quantal secretion from patch-clamped rat pancreatic β-cells. *J. Biol. Chem.* 271:270–277.

Zhu, H., B. Hille, and T. Xu. 2002. Sensitization of regulated exocytosis by protein kinase C. *Proc. Natl. Acad. Sci. USA*. 99:17055–17059.